Check for updates

A chemosensor with a paddle structure based on a BODIPY chromophore for sequential recognition of Cu²⁺ and HSO₃⁻†

Shengling Li,[a] Duanlin Cao,[a] Zhiyong Hu,[ab] Zhichun Li,[a] Xianjiao Meng,[a] Xinghua Han[ab] and Wenbing Ma ⓘ *[ab]

In this study, a highly selective chemosensor **ML** based on a BODIPY fluorescent chromophore was synthesized for sequential recognition of Cu²⁺ and HSO₃⁻ in a CH₃OH/H₂O (99 : 1 v/v) system, which contained three recognition sites and its structure characterized by ¹H NMR, ¹³C NMR and ESI-HR-MS. The sensor **ML** showed an obvious "on–off" fluorescence quenching response toward Cu²⁺ and the **ML**-Cu²⁺ complex showed an "off–on" fluorescence enhancement response toward HSO₃⁻. The detection limit of the sensor **ML** was 0.36 μM to Cu²⁺ and 1.4 μM to HSO₃⁻. In addition, the sensor **ML** showed a 1 : 3 binding stoichiometry to Cu²⁺ and the recovery rate of **ML**-Cu²⁺ complex identifying HSO₃⁻ could be over 70%. Sensor **ML** showed remarkable detection ability in a pH range of 4–8.

Introduction

Copper is an essential trace element for organisms and plays an important role in various biological processes such as catalysis of enzymes, gene expression and protein synthesis.[1–5] Under normal conditions, the allowable limit of Cu²⁺ is 15.7–23.6 μM in blood and 20–30 μM in drinking water, respectively.[6,7] A moderate concentration of Cu²⁺ is helpful to maintain the normal function of the body, but an excess concentration of Cu²⁺ may cause many neurological complications such as Wilson's disease and Alzheimer's disease.[8–11] Therefore, it is imperative to develop a simple, rapid and sensitive analytical method for detecting Cu²⁺. Some fluorescent sensors can identify metal ions selectively and colorimetrically[12,13] and have many advantages such as high selectivity and sensitivity, simple operation and low cost, making them attractive in the detection of Cu²⁺.[14–19]

SO₂ is the main component of acid rain as it can be dissolved in neutral aqueous solution to form a mixed system with a HSO₃⁻ to SO₃²⁻ molar ratio of about 3 : 1.[20–23] HSO₃⁻ plays an important role in both enzymatic and non-enzymatic reactions, and it is widely used as preservatives in foods and beverages.[24,25] However, excessive intake of HSO₃⁻ can not only cause damage to tissues, cells and biological macromolecules, but also can cause respiratory disease and many neurological disorders.[26–28] The acceptable daily intake of HSO₃⁻ should be less than 0.7 mg kg⁻¹ of body weight[29] and the sulfite content in foods and beverages should be less than 125 μM.[24] In recent years, fluorescent sensors have been developed using different approaches for detecting HSO₃⁻, such as coordination to metal ions,[30] selective reaction with aldehyde,[31,32] selective deprotection of levulinate group[33,34] and Michael-type addition.[35–37] However, there are few reports on the development of chemical sensors that can sequentially identify metal ions and HSO₃⁻ and simultaneously avoid interference by other sulfur-containing compounds. Clearly, it is more efficient and cost effective to sequentially identify metal ions and anions in practical applications.

BODIPY fluorescent dye is often used as a chromophore for the design and synthesis of fluorescent sensors because of its high molar extinction coefficient, high fluorescence quantum yield, good photothermal stability, easy structural modification and adjustable absorption and emission wavelengths to the infrared visible region.[38–42] In this study, we synthesized a chemosensor **ML** with a paddle structure[43,44] and three metal ion recognition sites by introducing three BODIPY fluorescent chromophores. This sensor showed an "on–off–on" fluorescence response to Cu²⁺ and HSO₃⁻ in CH₃OH/H₂O (99 : 1 v/v) system. Importantly, the colour of the test solution changed obviously, indicating that the sensor **ML** could be used for naked eye detection of Cu²⁺ and HSO₃⁻ (Scheme 1).

Experimental

Materials and methods

Compound **1** and **2** were synthesized as described in previous studies.[45,46] Other solvents and starting materials were purchased from Aladdin and Energy Chemical Reagents Ltd.

[a]School of Chemical Engineering and Technology, North University of China, Taiyuan 030051, P. R. China. E-mail: mawenbing@nuc.edu.cn

[b]National Demonstration Center for Experimental Comprehenisve Chemical Engineering Education, North University of China, Taiyuan 030051, P. R. China

† Electronic supplementary information (ESI) available. See DOI: 10.1039/c9ra08345f
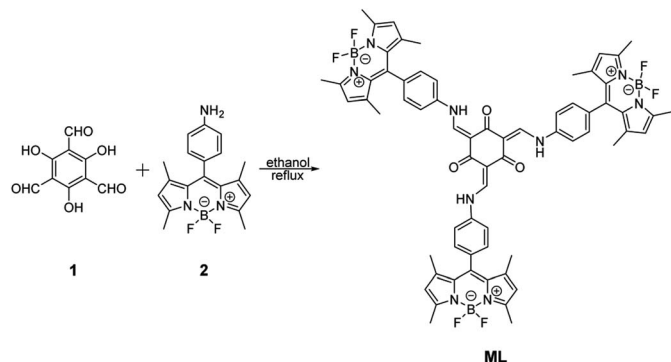
Scheme 1 Synthesis of sensor molecule **ML**.

Ultrapure water was used through all the tests. The pH of all solutions was adjusted on a PHS-3C pH meter (Shanghai, China). The ^{1}H NMR (400 M) and ^{13}C NMR (100 M) spectra were recorded on a spectrometer (Switzerland) in CDCl$_3$-d and DMSO-d_6 solutions. The SEI-MS spectra of sensor **ML** was recorded on a Bruker Solarix XR Fourier transform-ion cyclotron resonance (FT-ICR) mass spectrometer. The UV-spectras of all samples were recorded on a UV-2602 spectrophotometer (Shanghai, China), and all fluorescence spectras were recorded on a Hitachi F-2500 spectrophotometer (Japan).

Synthesis

Preparation of sensor ML. A 50 mL round-bottomed flask containing compound **1** (0.2 mmol, 42 mg), compound **2** (0.62 mmol, 210 mg), 20 mL absolute ethanol and a drop of glacial acetic acid was heated to reflux for 12 h and TLC monitoring. The mixture was cooled to room temperature, filtered, and washed with ice ethanol, and the filter cake was purified by silica gel column chromatography (petroleum ether : ethyl acetate = 5 : 1–1 : 1) to afford an orange solid (172 mg, 73%). ^{1}H NMR (CDCl$_3$-d, 400 MHz, TMS): δ (ppm) 13.45–13.53 (m, 2H), 13.10–13.14 (m, 1H), 8.81–8.92 (m, 3H), 7.45–7.50 (m, 6H), 7.35–7.40 (m, 6H), 6.01 (s, 6H), 2.57 (s, 18H), 1.46 (s, 18H). ^{13}C NMR (CDCl$_3$-d, 100 MHz, TMS): δ (ppm): 185.5, 155.9, 149.2, 142.8, 140.2, 139.7, 132.4, 131.4, 130.0, 121.5, 118.3, 107.2, 14.7, 14.6. The NMR spectra of sensor **ML** were shown in Fig. S1 and S2.† HRMS (ESI): m/z calcd for C$_{66}$H$_{61}$B$_3$F$_6$N$_9$O$_3$ [(M + H)$^+$]: 1174.5083, found 1174.5103 (Fig. S3†).

### General procedure for fluorescence spectra experiments

In this study, sixteen kinds of metal cations and thirteen kinds of anions were selected. Cations included: K$^+$, Ca^{2+}, Na$^+$, Li$^+$, Mg^{2+}, Zn^{2+}, Fe^{3+}, Cu^{2+}, Al^{3+}, Ag$^+$, Hg^{2+}, Cs$^+$, Pb^{2+}, Cd^{2+}, Ba^{2+} and Ni^{2+}; anions included: F$^-$, Cl$^-$, Br$^-$, I$^-$, OAc$^-$, HCO$_3^-$, CO$_3^{2-}$, HSO$_3^-$, SO$_3^{2-}$, SO$_4^{2-}$, S^{2-}, NO$_3^-$ and NO$_2^-$. All tests were carried out at room temperature (25 °C) in CH$_3$OH/H$_2$O (99 : 1 v/v) system. The UV-vis absorption spectra and fluorescence spectra of sensor **ML** at a concentration of 5×10^{-6} M were recorded and the excitation wavelength was 475 nm, the slits of emission and excitation were 5 nm in all experiments. The stock solutions of various metal ions and anions (1×10^{-2} M) were prepared from chlorine and sodium salts in ultrapure water, respectively.

Results and discussion

UV and fluorescence response of sensor ML towards Cu^{2+}

The UV-vis spectra of sensor **ML** and 10 equiv. different metal ions responses were shown in Fig. 1. The sensor **ML** showed no response to metal ions except Cu^{2+}. The maximum absorption wavelength showed a significant red shift from 499 nm to 510 nm with a red shift of 11 nm, and the absorbance was also significantly reduced. The color of the solution changed from yellow to pink, indicating that the sensor **ML** could be used for naked eye recognition of Cu^{2+}.

Fig. 2 showed that as the Cu^{2+} concentration increased, the absorbance decreased gradually and the absorption peak became wider. The maximum absorption wavelength shifted from 499 nm to 510 nm, and the color of the solution changed gradually from yellow to pink. The sensor **ML** coordinated with Cu^{2+} to form a stable complex, resulting in a decrease in the intensity of its UV-vis spectrum and a red shift. The five equal concentration points were observed at 339 nm, 378 nm, 444 nm,
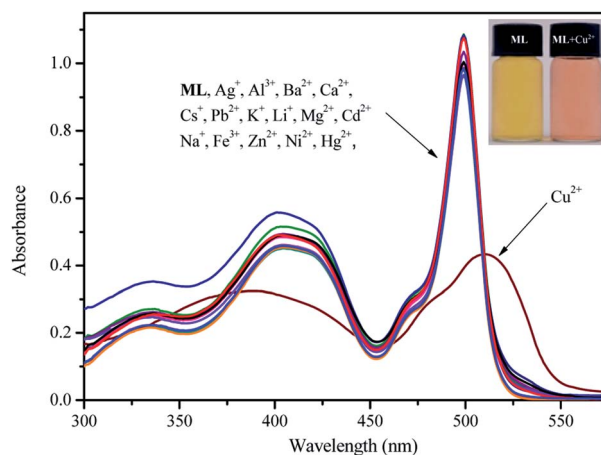
Fig. 1 UV-vis spectra of sensor **ML** in CH$_3$OH/H$_2$O (99 : 1 v/v) system with the addition of 10 equiv. of metal ions and blank.
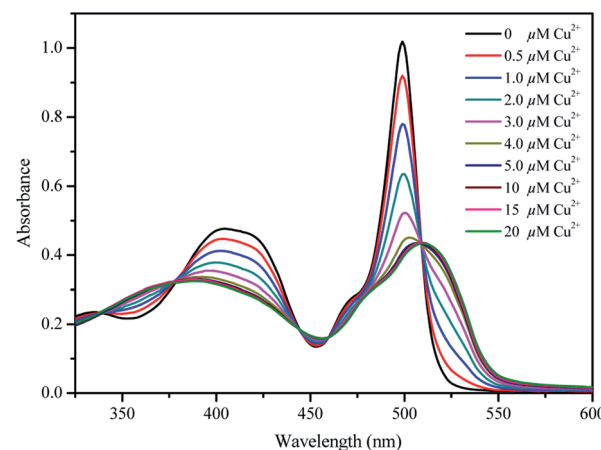
Fig. 2 UV-vis spectra of sensor **ML** of various concentrations [0 μM, 0.5 μM, 1.0 μM, 2.0 μM, 3.0 μM, 4.0 μM, 5.0 μM, 10 μM, 15 μM, 20 μM Cu^{2+}] in CH$_3$OH/H$_2$O (99 : 1 v/v) system.

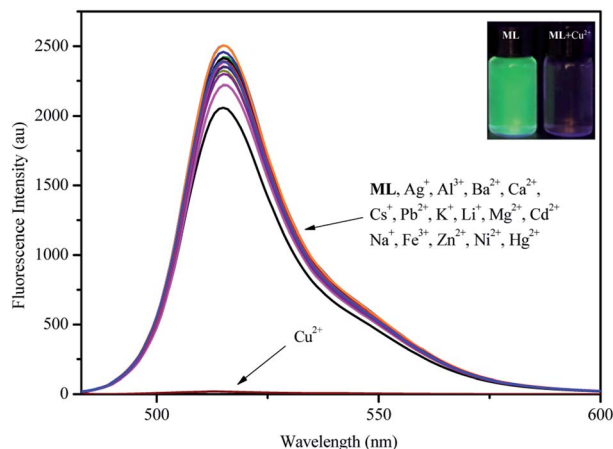**Fig. 3** Fluorescence spectra of sensor **ML** in CH_3OH/H_2O (99 : 1 v/v) system at an excitation of 475 nm with the addition of 10 equiv. of metal ions and blank.

Fig. 5 Fluorescence spectra of **ML**-Cu^{2+} (5 μM) complex with the addition of 10 equiv. different anions in CH_3OH/H_2O (99 : 1 v/v) system.

460 nm and 509 nm, respectively, indicating that the sensor **ML** and the complex **ML**-Cu^{2+} were in a dynamic equilibrium.

Fig. 3 showed that the addition of Cu^{2+} resulted in almost complete quenching of the fluorescence intensity of the sensor **ML**, but only a slight change in the fluorescence intensity of other metal ions. The maximum emission wavelength was 515 nm and the Stokes shift was 40 nm, and thus the sensor **ML** showed good selectivity to Cu^{2+} in CH_3OH/H_2O (99 : 1 v/v) system at an excitation of 475 nm. As shown in Fig. S4,† the fluorescence spectras with the presence of other metal cations were almost the same as that with the presence of only Cu^{2+}, which also indicated that the detection of Cu^{2+} would not be affected by the presence of other metal cations.

Fig. 4 showed that as the Cu^{2+} concentration increased, the fluorescence intensity of the sensor **ML** decreased gradually. At a Cu^{2+} concentration of 8 equiv., the fluorescence intensity was approximately zero and the quenching rate was above 90%, indicating that the sensor **ML** was highly sensitive to Cu^{2+}. The
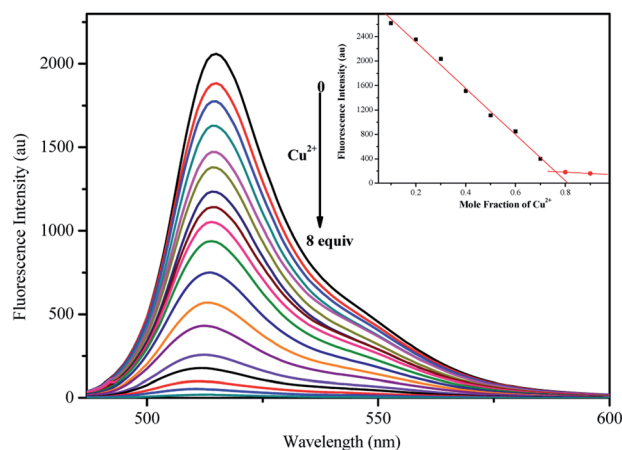

Fig. 6 Fluorescence spectra of 5 μM **ML**-Cu^{2+} in the presence of various concentrations of HSO_3^- in CH_3OH/H_2O (99 : 1 v/v) system at an excitation of 475 nm.

Fig. 4 Fluorescence spectra of 5 μM sensor **ML** with the addition of various concentrations of Cu^{2+} in CH_3OH/H_2O (99 : 1 v/v) system at an excitation of 475 nm. The inset plots showed that sensor **ML** formed a 1 : 3 complex with Cu^{2+}.
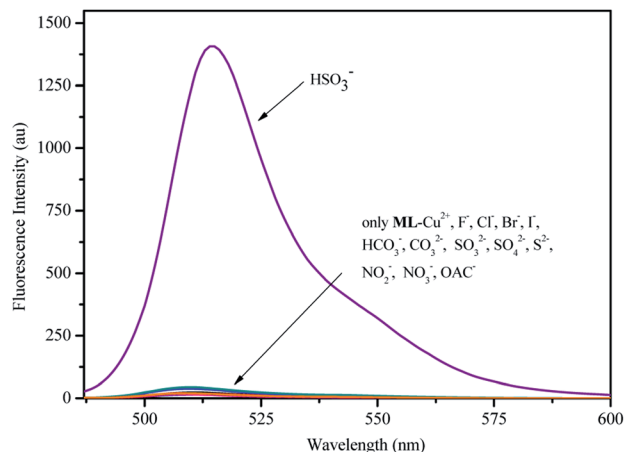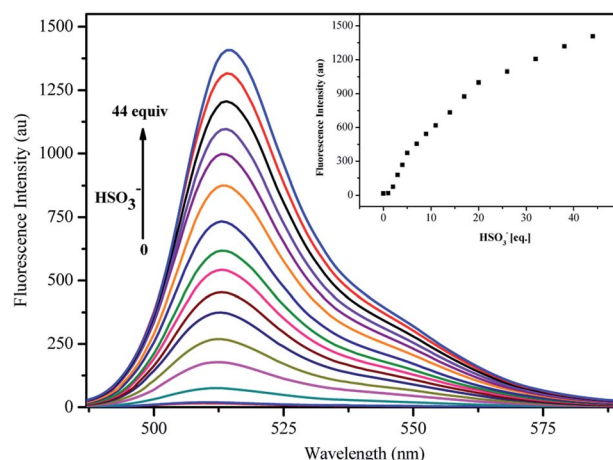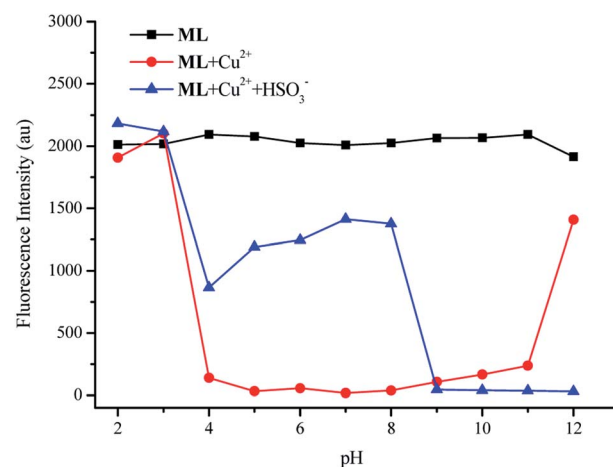

Fig. 7 Changes of the fluorescence intensity of sensor **ML** towards Cu^{2+} (10 equiv.) and HSO_3^- (10 equiv.) over a wide range of pH in CH_3OH/H_2O (99 : 1 v/v) system at room temperature.

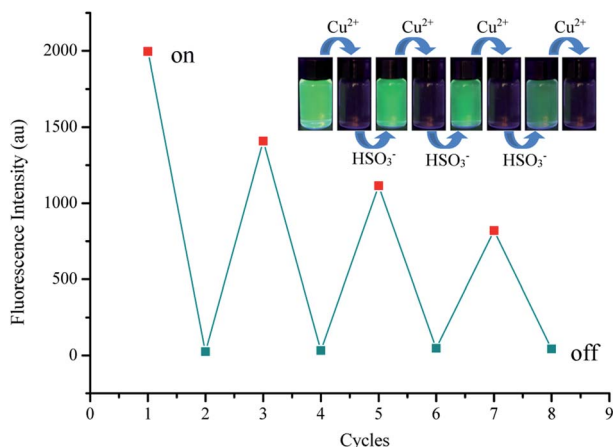**Fig. 8** The sequential recognition of sensor **ML** (10 μM) upon alternate addition of Cu^{2+} and HSO_3^- in CH_3OH/H_2O (99 : 1 v/v) system (λ_{ex} = 475 nm).

binding constant K_a was determined to be 1.70×10^4 M^{-1} (R^2 = 0.99675, Fig. S5†) and the detection limit was calculated to be 0.36 μM by LOD = $3\sigma/m$ (Fig. S6†). The Job curve at the upper right corner showed that the inflection point was observed at a Cu^{2+} concentration of 0.76 equiv., indicating that the coordination ratio of the sensor **ML** and Cu^{2+} was 1 : 3.

Fluorescence response of ML-Cu^{2+} complex towards HSO_3^-

The complex formed by the sensor **ML** and Cu^{2+} was used as a new sensor **ML**-Cu^{2+} for sequential recognition of anions. As shown in Fig. 5, the fluorescence intensity was enhanced after the addition of anions containing HSO_3^-, but remained unchanged after the addition of other anions. The fluorescence was recovered to a large extent after adding HSO_3^- with a response rate of 70%, indicating that the new sensor could identify HSO_3^- specifically. As shown in Fig. S7,† the addition of HSO_3^- to **ML**-Cu^{2+} containing other anions still resulted in an obvious enhance in the fluorescence response. Thus, the sensor **ML**-Cu^{2+} was not

interfered by other anions, and the interference of other sulfur-containing anions was also excluded, which further indicated that the **ML**-Cu^{2+} had good selectivity to HSO_3^-.

It could be seen from Fig. 6 that the intensity of the strongest fluorescence emission peak gradually increased with the increase of HSO_3^- concentration to 44 equiv., after which the intensity remained largely unchanged. Furthermore, the detection limit was 1.4 μM according to the formula LOD = $3\sigma/m$ (Fig. S8†).

Effect of pH

Fig. 7 showed that the fluorescence of sensor **ML** was quenched after the addition of Cu^{2+} at pH = 4–11, and sensor **ML** could sequentially recognize Cu^{2+} and HSO_3^- at pH = 4–8. It might be that the disruption of the structure of sensor **ML** under strong acid and alkali conditions affected the coordination ability of sensor **ML** with ions. Furthermore, HSO_3^- and OH^- could not coexist in a large amount under alkaline conditions, so sensor **ML** had no recognition response to HSO_3^- at pH = 9–12.

Reversibility of sensor ML for Cu^{2+} and HSO_3^-

The stability of sensor **ML** in identifying Cu^{2+} and HSO_3^- was discussed with Cu^{2+} and HSO_3^- as input signals and fluorescence intensity as output signals. As shown in Fig. 8, the fluorescence intensity quenched by Cu^{2+} still remained stable after four cycles; the recovery rate of the fluorescence intensity after the first addition of HSO_3^- was above 70%, and then the three recovery rates gradually decreased. The figure at the upper right corner showed that the sensor **ML** could be used to sequentially identify Cu^{2+} and HSO_3^- in practical applications.

The possible mechanism of sensor ML for Cu^{2+} and HSO_3^-

The Job curve showed that the coordination ratio of sensor **ML** to Cu^{2+} was 1 : 3. The sensor **ML** provided three coordination
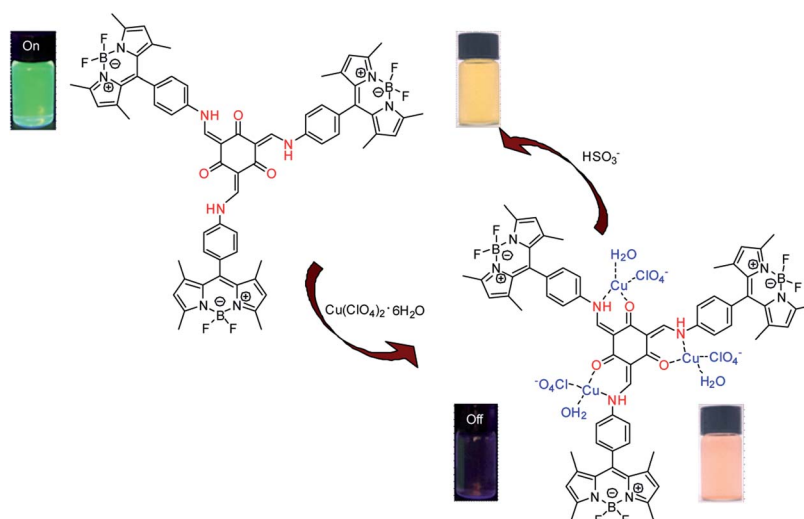
Scheme 2 The possible mechanism of **ML**-Cu^{2+} with HSO_3^-.

points through the three O atoms on the carbonyl group and the three N atoms at the –NH-position to form a metal copper by 1 : 3 bonding with Cu^{2+}. This sensor **ML** showed an "on–off–on" fluorescence response to Cu^{2+} and HSO_3^- in CH_3OH/H_2O (99 : 1 v/v) system.

In order to better understand the binding mode between sensor **ML** and Cu^{2+}, the ^{1}H NMR titration experiments were conducted as showed in Fig. S9.† As the Cu^{2+} concentration increased, the N–H signals gradually disappeared with respect to sensor **ML**. The broadening of signals could also be affected by coordination. The molecular ion peak (ESI-MS) at 1713.14284 [sensor **ML** + $3Cu^{2+}$ + $3ClO_4^-$ + $3H_2O$; m/z calcd for 1713.16792] (see Fig. S10†) indicated an approximately 1 : 3 complexation between sensor **ML** and Cu^{2+}. Based on the analysis of Job's plot, mass spectrometry and ^{1}H NMR, the possible coordination mode was shown in Scheme 2.

Conclusions

In this study, sensor **ML** was successfully synthesized for sequential recognition of Cu^{2+} and HSO_3^-. Sensor **ML** showed an obvious "on–off" fluorescence quenching response toward Cu^{2+} with a quenching efficiency of above 90%, and the colour of the solution changed from yellow to pink. The **ML**-Cu^{2+} complex could be used to identify HSO_3^- selectively with a recovery rate of above 70%. Sensor **ML** showed a 1 : 3 binding stoichiometry to Cu^{2+} with a complexation constant of $1.70 \times 10^4 \text{ M}^{-1}$. The detection limits for Cu^{2+} and HSO_3^- were calculated to be 0.36 μM and 1.4 μM, respectively. The stable pH range of sensor **ML** to Cu^{2+} and **ML**-Cu^{2+} to HSO_3^- was from 4 to 8.

Conflicts of interest

There are no conflicts to declare.

Acknowledgements

Notes and references

1 H. M. Kang, C. B. Fan, H. T. Xu, G. Liu and S. Z. Pu, *Tetrahedron*, 2018, **74**, 4390–4399.

2 H. Wang, B. Fang, L. Zhou, L. Di, K. Lin, U. Kajsa and Z. J. Hu, *Org. Biomol. Chem.*, 2018, **16**, 2264–2268.

3 M. A. Cardona, M. Kveder, U. Baisch, M. R. Sensorrt and D. C. Magriet, *RSC Adv.*, 2016, **6**, 84712–84721.

4 K. K. Liu, L. N. Zhang, L. N. Zhu, R. Zhang, X. Z. Li and D. M. Kong, *Sens. Actuators, B*, 2017, **247**, 179–187.

5 Z. Y. Zhang, Y. P. Liu and E. J. Wang, *Dyes Pigm.*, 2019, **163**, 533–537.

6 H. S. Jung, P. S. Kwon, J. W. Lee, J. I. Kim, C. S. Hong, J. W. Kim, S. Yan, J. Y. Lee, J. H. Lee, T. Joo and J. S. Kim, *J. Am. Chem. Soc.*, 2009, **131**, 2008–2012.

7 B. Zhang, Q. P. Diao, P. Ma, X. Liu, D. Q. Song and X. H. Wang, *Sens. Actuators, B*, 2016, **225**, 579–585.

8 H. M. Kang, C. B. Fan, H. T. Xu, G. Liu and S. Z. Pu, *Spectrochim. Acta, Part A*, 2019, 322–329.

9 S. Erdemir and S. Malkondu, *Dyes Pigm.*, 2019, **163**, 330–336.

10 R. Squitti, M. Siotto, M. Arciello and L. Rossi, *Metallomics*, 2016, **8**, 863–873.

11 X. Tian, Z. P. Dong, J. R. Hou, R. Wang and J. T. Ma, *J. Lumin.*, 2014, **145**, 459–465.

12 Y. L. Fu, C. B. Fan, G. Liu and S. Z. Pu, *Sens. Actuators, B*, 2017, **239**, 295–303.

13 D. D. Xue, C. H. Zheng, S. Z. Qu, G. M. Liao, C. B. Fan, G. Liu and S. Z. Pu, *Luminescence*, 2017, **32**, 652–660.

14 X. J. Meng, D. L. Cao, Z. Y. Hu, X. H. Han, Z. C. Li, D. Liang and W. B. Ma, *Tetrahedron Lett.*, 2018, **59**, 4299–4304.

15 S. L. Li, H. C. Ding, Y. S. Wang, C. B. Fan, G. Liu and S. Z. Pu, *RSC Adv.*, 2019, **9**, 6643–6649.

16 J. Wang, J. Liang, X. Liu, X. Han, F. P. Dong, Y. L. Wang, X. Shu, F. R. Huang and H. B. Liu, *Spectrochim. Acta, Part A*, 2019, **215**, 260–265.

17 J. B. Qiu, S. J. Jiang, B. N. Lin, H. Y. Guo and F. F. Yang, *Dyes Pigm.*, 2019, **170**, 107590.

18 Z. P. Meng, S. L. Wu, L. H. Zhong, M. Zeng, X. Q. Sun, L. Li and S. F. Zhang, *RSC Adv.*, 2018, **8**, 38075–38080.

19 S. L. Guo, G. Liu, C. B. Fan and S. Z. Pu, *Sens. Actuators, B*, 2018, **266**, 603–613.

20 Y. T. Yang, B. Z. Bai, W. Z. Xu, Z. D. Xu, J. C. Zhang and W. Li, *Dyes Pigm.*, 2017, **136**, 830–835.

21 J. W. Shi, W. Shu, Y. Tian, Y. L. Wu, J. Jing, R. B. Zhang and X. L. Zhang, *RSC Adv.*, 2019, **9**, 22348–22354.

22 H. D. Li, Q. C. Yao, J. L. Fan, C. Hu, F. Xu, J. J. Du, J. Y. Wang and X. J. Peng, *Ind. Eng. Chem. Res.*, 2016, **55**, 1477–1483.

23 X. L. Zheng, H. Li, W. Feng, H. C. Xia and Q. H. Song, *ACS Omega*, 2018, **3**, 11831–11837.

24 J. L. Wang, Y. F. Hao, H. Wang, S. X. Yang, H. Y. Tian, B. G. Sun and Y. G. Liu, *J. Agric. Food Chem.*, 2017, **65**, 2883–2887.

25 F. Zhou, Y. Sultanbawa, H. Feng, Y. L. Wang, Q. T. Meng, Y. Wang, Z. Q. Zhang and R. Zhang, *J. Agric. Food Chem.*, 2019, **67**, 4375–4383.

26 J. Lu, P. Wu, Y. X. Geng and J. C. Wang, *RSC Adv.*, 2018, **8**, 33459–33463.

27 J. B. Chao, H. J. Wang, Y. B. Zhang, C. X. Yin, F. J. Huo, J. Y. Sun and M. G. Zhao, *New J. Chem.*, 2018, **42**, 3322–3333.

28 D. Don, K. Velmurugan, J. Prabhu, N. Bhuvanesh, A. Thamilselvan and R. Nandhakumar, *Spectrochim. Acta, Part A*, 2017, **174**, 62–69.

29 L. Zou, G. Zhang, M. H. Zhou, X. Xin, S. Chen, X. M. Duan and J. K. Xu, *Ind. Eng. Chem. Res.*, 2019, **58**, 9231–9238.

30 X. H. Li, R. Q. Zeng, C. Y. Xie, D. G. Tang, Q. Li, B. G. Zhang and T. Huang, *Dyes Pigm.*, 2019, **165**, 128–136.

31 S. Xu, R. R. Tang, Z. Wang, Y. Zhou and R. Yan, *Spectrochim. Acta, Part A*, 2015, **149**, 208–215.

32 X. H. Cheng, H. Z. Jia, J. Feng, J. G. Qin and Z. Li, *Sens. Actuators, B*, 2013, **184**, 274–280.

33 M. G. Choi, J. Hwang, S. Eor and S. K. Chang, *Org. Lett.*, 2010, **12**, 5624–5627.

34 X. Ma, C. X. Liu, Q. L. Shan, G. H. Wei, D. B. Wei and Y. G. Du, *Sens. Actuators, B*, 2013, **188**, 1196–1200.

35 J. Li, Y. Gao, H. R. Guo, X. K. Li, H. Y. Tang, J. Li and Y. Guo, *Dyes Pigm.*, 2019, **163**, 285–290.

36 K. Y. Bi, R. Tan, R. T. Hao, L. X. Miao, Y. Q. He, X. H. Wu, J. F. Zhang and R. Xu, *Chin. Chem. Lett.*, 2019, **30**, 545–548.

37 X. H. Pan, Y. Zhong, Y. S. Jiang, G. C. Zuo, J. J. Li and W. Dong, *Mater. Chem. Phys.*, 2018, **213**, 83–88.

38 Y. Huang, C. F. Li, W. J. Shi, H. Y. Tan, Z. Z. He, L. Y. Zheng, F. G. Liu and J. W. Yan, *Talanta*, 2019, **198**, 390–397.

39 Y. N. Li, L. Yang, M. Q. Du and G. J. Chang, *Analyst*, 2019, **144**, 1260–1264.

40 S. Jantra, P. Butta, P. Jithavech, P. Rojsitthisak, T. Palaga, P. Rashatasakhon, M. Sukwattanasinitt and S. Wacharasindhu, *Dyes Pigm.*, 2019, **162**, 189–195.

41 J. H. Ye, J. Xu, H. C. Chen and Y. Bai, *RSC Adv.*, 2014, **4**, 6691.

42 Y. Gawale, S. Mangalath, N. Adarsh, J. Joseph, D. Ramaiah and N. Sekar, *Dyes Pigm.*, 2019, **171**, 107684.

43 M. Xu, C. X. Yin, F. J. Huo, Y. B. Zhang and J. B. Chao, *Sens. Actuators, B*, 2014, **204**, 18–23.

44 Y. P. Wang, D. L. Qiu, M. N. Li, Y. J. Liu, H. B. Chen and H. M. Li, *Spectrochim. Acta, Part A*, 2017, **185**, 256–262.

45 Y. J. Cheng, R. Wang, S. Wang, X. J. Xi, L. F. Ma and S. Q. Zang, *Chem. Commun.*, 2018, **54**, 13563–13566.

46 T. Matsumoto, Y. Urano, T. Shoda, H. Kojima and T. Nagano, *Org. Lett.*, 2007, **9**, 3375–3377.